

Chapter 1. Laser induced optical breakdown

1.1 Energy deposition in laser irradiated materials

“The history of laser-induced breakdown is almost as old as the history of the laser itself” [Blo74]

The goal of this chapter is to introduce the main mechanisms for energy absorption (with the result in rapid build up of free carriers), and deposition (coupling with the lattice subsystem) in laser irradiated dielectric materials, when the photon energy is small compared to the material band-gap.

A quantitative estimation of the energy transport in laser irradiated transparent materials has to take into account the fact that laser radiation interacts primarily with the electronic system.

The deposited energy is then transferred to the lattice as heat via collisions with phonons. For very short pulses both processes can be temporarily decoupled (although some phonons can be created in the process of laser absorption by electrons, the main energy transfer takes place from the hot electron sink after the pulse has stopped).

For pulses longer than a few tens of picoseconds, the generally accepted picture of laser damage/ablation involves the heating of conduction band electrons by the incident radiation and transfer of this energy to the lattice in a quasi-equilibrium, steady-state fashion during the laser pulse (in a photon-electron-phonon and electron-phonon interaction). Damage occurs via conventional heat deposition resulting in a phase transformation of the dielectric material [JBC89, ArC92].

In order to reach the breakdown level, the transparent, dielectric, material has to be initially transformed into an absorber, so a high density of electrons (around the critical density) have to be “pumped” into the conduction band. Therefore the theories of laser induced damage must explain the primary process of production of sufficient free-carriers for efficient light absorption into the initially transparent solid and then the energy deposition to the lattice. The basic channels for free-electron generation in the presence of intense optical fields were identified either in (a) multiphoton interband transitions or in (b) electron impact (avalanche) ionization [Yab71, Blo74, JBC89, SFR95, TBK99]. In this respect the multiphoton theory is somewhat straightforward in principle but the multiphoton cross

1.1 Energy deposition in laser irradiated materials

sections are rather small and difficult to calculate, while the avalanche theory must explain the energy gain of the free electron in the high frequency electric field in sufficient quantity to liberate another electron from the valence band and place it in the conduction band. The solution has been identified in the possibility of fast momentum change by collisions so that the electrons will be synchronized with the field oscillations (i.e. will maintain the appropriate phase relations with the electric field) and the average energy gain would be nonzero [JBC89 and references therein].

The main experimental approach in determining the optical breakdown conditions for transparent materials is given by optical damage measurements [MaP86, SFH96, DLK94, and VAR96] at different pulse durations. Thermal effects have been observed for pulses longer than 20 ps, below this value a deviation from the thermally induced $\tau_L^{1/2}$ dependency of the optical damage threshold on the pulse duration τ_L is seen [SFR95].

Jones et al. [JBC89] among others, have also underlined the role of investigations of pre-breakdown phenomena, especially the build up and temporal behavior of the electronic population [JBC89, QGM99], trapping and defect formation [JBC89, SaG93, PDG96] or lattice heating at subthreshold laser intensities [JBC89]. High order excitation has been evidenced as expected for multiphoton transitions [QGM99], with strong absorption very close to the damage threshold [JCB89] reinforcing the idea of avalanche breakdown. However, since in the case of an avalanche mechanism, the absorption would be effective only at the threshold, the pre-breakdown investigations can offer only a very limited quantity of information on electron impact ionization.

Historically, the optical damage threshold experimental approach turned out to be difficult to realize in order to obtain reliable data describing an “intrinsic” threshold free of external causes [MaP86, JBC89].

The initial, early, predictions have emphasized that avalanche processes are mainly responsible for optical damage of different transparent materials [Blo74, Yab71], especially at IR and NIR wavelengths, based on arguments related to the statistical character of laser induced damage threshold, similarities with DC threshold and reduced sensitivity to the laser wavelength up to the visible region. The main idea relied on the statistical presence of a small number of free electrons in the conduction band within the irradiated volume to initiate the avalanche. This explains the probabilistic character of the breakdown threshold, with a large interval of possible values in similar conditions. For nanosecond pulses, the threshold does not have a sharp, well-defined character. Instead, a probability distribution can be defined with a probability for breakdown increasing from zero to unity in an interval of electric field

values. This accounts for the spread in the experimental values. The simple avalanche picture has been criticized and the discussion has been completed with additional effects like free-electron heating (photon absorption by free electrons with creation of phonons for momentum conservation and subsequent lattice heating) or polaron heating [ArC92, MaP86, JBC89 and references therein]. The idea of a statistical model of damage based on the probability of liberating one or a few starting electrons to initiate the avalanche has now been abandoned, and it has been concluded that even large order multiphoton absorption can provide a large number of starting electrons [JBC89].

The availability of ultrashort pulsed lasers for applications in material processing has emphasized this picture in the sense that multiphoton ionization is greatly enhanced and the generation of electrons in the conduction band does not rely on an arbitrary number of initial “seed“ electrons. This leads to better control in the processing parameters and decreases the fluctuations associated with the ablation threshold [SFR95, SFH96, DLK94, and DLM96]. Because there are no statistical fluctuations in the number of starting electrons, a sharp, intrinsic, material damage threshold can be defined.

Multiphoton induced free electrons are rapidly heated in the laser field and multiplied by an avalanche mechanism. The electrons gain energy in the field of an ultrashort laser pulse generally much faster than they are able to transfer energy to the lattice. All processes related to optical damage and ablation occur after the pulse has passed, when the electron energy is coupled into the lattice. Thus, during the pulse, there is no appreciable heating of the lattice and, hence, no significant change in the electron-lattice scattering rates. Also thermal and mechanical stresses are greatly reduced.

Any attempt to model the occurrence of optical damage and ablation should address the following points:

- the mechanism of laser absorption and the balance between multiphoton/tunnel ionization and impact ionization.
- electron-electron thermalization and the energy redistribution
- photoelectron emission and surface charging
- electron trapping and the characteristic times in traps as precursors to stable defects
- defect formation and incubation
- electron-phonon inelastic scattering and lattice heating
- lattice thermalization and phase transformation

Typically, the description of the electron avalanche development is based on the solution of a kinetic equation for the electron distribution function. A Fokker-Plank equation

1.1 Energy deposition in laser irradiated materials

is used to describe the temporal behavior of the number density of the electrons $f(\varepsilon, t)d\varepsilon$ with a kinetic energy between ε and $\varepsilon+d\varepsilon$ at time t for dielectrics with the band-gap energy (U_I) much higher than the photon energy ($h\nu$).

A detailed description of the avalanche process using the Boltzmann transport equation would involve a complete knowledge of all electron and phonon collision processes including energy dependencies of the excitation and ionization cross sections, difficult to predict in condensed matter. It is nevertheless possible to understand the general characteristics of the breakdown phenomenon recognizing that the electron density will increase since some electrons will be accelerated to energies higher than the band-gap.

The problem of electron transport and impact ionization in the case of dielectrics subject to high laser fields has been extensively addressed in the literature (see [ArC92, TBK99] and references therein) and elaborate calculations and computer assisted simulations have been performed [ArC92]. Some of the aspects such the relative balance between the different channels for free electron production and lattice heating (multiphoton ionization, impact ionization, free-electron heating, electron-phonon scattering) as well as the exact dependencies for the parameters involved (avalanche ionization rates and the electron distribution functions) are still under discussion. As we have stated before, the intention of this chapter is to present an intuitive analytical formalism which is illustrative for the mechanism of laser coupling to transparent materials and subsequent damage and which is also in good agreement with the observed experimental behavior [SFH96].

Below is given a general mathematical description of the avalanche process as responsible for optical damage of transparent materials in intense laser fields.

The main channels for accumulation and energy redistribution will be presented in connection with the development of a significant free electron population. Energy dispersion and the temporal behavior of these channels will be underlined.

The idea is to show that an analytical expression for the avalanche rate can be derived, displaying a simple laser intensity dependence. This will find application in a simple rate equation for the electron population to describe the avalanche process.

This is the consequence of two major assumptions, which will be developed below:

1. Flux doubling (i.e. as soon as the electron reaches an energy sufficient to ionize, a second electron is generated by impact ionization and both electrons are left at zero energy).
2. During the avalanche, the energy distribution of the electrons grows in magnitude without changing shape.

The model which follows has been developed by Holway [Hol72, Hol74], and Holway and Frandin [HoF75] based on previous theories of electron multiplication and dielectric breakdown by Seitz and Fröhlich [Sei49, FrS50] and transport equations by Uhlenbeck and Orstein [UhO30] and refined by Stuart et al. [SFH96].

We have decided to follow the argumentation presented by Stuart et al. [SFH96]. This produces an intuitive and straightforward outcome in an analytical form.

The Fokker-Plank equation has been developed from the Boltzmann transport equation [Hol74] with no source term involved.

$$\frac{\partial f(\varepsilon, t)}{\partial t} = -\frac{\partial}{\partial \varepsilon} \left[\frac{\langle \Delta \varepsilon \rangle}{\Delta t} f \right] + \frac{1}{2} \frac{\partial^2}{\partial \varepsilon^2} \left[\frac{\langle (\Delta \varepsilon)^2 \rangle}{\Delta t} f \right] = 0 \quad \text{E 1.1-1}$$

where:

$$\frac{\langle \Delta \varepsilon \rangle}{\Delta t} = A(\omega) Y(\omega) - \left(\frac{d\varepsilon}{dt} \right)_L \quad \text{E 1.1-2}$$

and,

$$\frac{\langle (\Delta \varepsilon)^2 \rangle}{\Delta t} = \frac{4}{3} \varepsilon A(\omega) \quad \text{E 1.1-3}$$

where,

$$A = \frac{e^2 E^2}{m} \left(\frac{v(\varepsilon)}{[v^2(\varepsilon) + \omega^2]} \right), \quad \text{E 1.1-4}$$

$$\left(\frac{\partial \varepsilon}{\partial t} \right)_L = U_{phon} \gamma(\varepsilon) \quad \text{E 1.1-5}$$

represents the losses by exciting phonons (optical and acoustic modes, depending on the free electron energy, and from here, energy dependent relaxation times, as a function of the electron position in the conduction band), and Y is given by:

$$Y = 1 + \frac{2}{3} \frac{\omega^2 - v^2}{\omega^2 + v^2} \left(\frac{\varepsilon}{v} \right) \frac{\partial v}{\partial \varepsilon} \quad \text{E 1.1-6}$$

The electron energy ε is measured with respect to the bottom of the conduction band, E is the electric field oscillating at frequency ω ($E = [2I / (\varepsilon_0 c n)]^{1/2}$ with n the refractive index, ε_0 the vacuum permittivity, I the laser intensity, and c the velocity of light) U_{phon} is the characteristic phonon energy, and $\gamma(\varepsilon)$ is the rate at which electron energy is transferred to the

1.1 Energy deposition in laser irradiated materials

lattice. The quantity $\nu=1/\tau_m(\epsilon)$ is the transport (momentum) scattering rate (with both polar and non-polar components).

$$\frac{1}{\tau_m} = \nu \propto \sum a_{pol/non-pol} \epsilon^{k_{pol/non-pol}} \quad \text{E 1.1-7}$$

Both $\tau_m(\epsilon)$ and $\gamma(\epsilon)$ are energy dependent (e.g. they vary by two orders of magnitude for energies in the conduction band in the case of fused silica [SFH96]).

The space diffusion of the carriers can be neglected for times less than 10^{-10} s (in the range of nanometers, much less than the laser focal dimensions), although evidence of ballistic effects for the electrons has been seen for metal targets [HMW97].

The first term in the right part of Eq. E 1.1-1 ($\langle \Delta \epsilon \rangle / \Delta t$) represents the average rate of change in energy for the average electron (gain in the electric field and losses by exciting phonons) and the second term ($\langle (\Delta \epsilon)^2 \rangle / \Delta t$) is the dispersion.

The net number of electrons per unit volume whose energy increases from a value less than ϵ to a value greater than ϵ per unit time can be defined as the current in energy space $J(\epsilon)$.

Eq. E 1.1-1 can be written as:

$$\frac{\partial f(\epsilon, t)}{\partial t} + \frac{\partial J(\epsilon, t)}{\partial \epsilon} \equiv \frac{\partial f(\epsilon, t)}{\partial t} + \frac{\partial}{\partial \epsilon} \left[V(\epsilon) f(\epsilon, t) - D(\epsilon) \frac{\partial f(\epsilon, t)}{\partial \epsilon} \right] = 0 \quad \text{E 1.1-8}$$

or, more generally,

$$\frac{\partial f(\epsilon, t)}{\partial t} + \frac{\partial}{\partial \epsilon} \left[V(\epsilon) f(\epsilon, t) - D(\epsilon) \frac{\partial f(\epsilon, t)}{\partial \epsilon} \right] \equiv \frac{\partial f(\epsilon, t)}{\partial t} + \frac{\partial J(\epsilon, t)}{\partial \epsilon} = S(\epsilon, t) \quad \text{E 1.1-9}$$

where,

$$V(\epsilon) = R_J(\epsilon, t) - U_{phon} \gamma(\epsilon) = \frac{\sigma(\epsilon) E^2(t)}{3} - U_{phon} \gamma(\epsilon) \quad \text{E 1.1-10}$$

and

$$R_J(\epsilon, t) = \frac{1}{3} A(\epsilon, t) \quad \text{E 1.1-11}$$

The current $J(\epsilon)$ represents direct heating and energy loss, as well as an energy diffusion with the coefficient $D(\epsilon)$ which is proportional to both the conductivity and laser intensity.

R_J accounts for Joule heating of electrons in terms of the conductivity per electron $\sigma(\epsilon)$.

$$\sigma(\varepsilon) = \frac{e^2 \tau_m(\varepsilon)}{m^* [1 + \omega^2 \tau_m^2(\varepsilon)]} \quad \text{E 1.1-12}$$

$$D(\varepsilon) = \frac{2\sigma(\varepsilon)E^2\varepsilon}{3} \quad \text{E 1.1-13}$$

The final term in Eq. E 1.1-9 $S(\varepsilon, t)$ includes sources and sinks of electrons.

$$S(\varepsilon, t) = R_{imp}(\varepsilon, t) + R_{pi}(\varepsilon, t) \quad \text{E 1.1-14}$$

Impact ionization at rate R_{imp} was included assuming that excess kinetic energy is equally divided between the resultant electrons [HoF75].

$$R_{imp}(\varepsilon, t) = -v_i(\varepsilon)f(\varepsilon) + 4v_i(2\varepsilon + U_I)f(2\varepsilon + U_I) \quad \text{E 1.1-15}$$

The electron impact ionization rate $v_i(\varepsilon)$ was approximated by the Keldysh formula [Rid93] as $\zeta(\varepsilon/U_I)^2$ ($\zeta = 1.5 \times 10^{15} \text{ s}^{-1}$ [ACD92]). The factor of 4 in the second term of Eq. E 1.1-15 can be justified by integrating Eq E 1.1-15 over energy [SFH96]. This shows that the net rate of electron production is simply $\int v_i(\varepsilon)f(\varepsilon)d\varepsilon$. The source term also includes multiphoton ionization at rate $R_{pi}(\varepsilon, t)$. The boundary conditions for Eq. E 1.1-9 require the vanishing of the distribution at $\varepsilon = \infty$ and the current at $\varepsilon = 0$.

Due to the rapid growth of the impact ionization rate for energies above the band gap, some researchers have replaced the source term $R_{imp}(\varepsilon, t)$ in Eq. E 1.1-15 by the boundary conditions:

$$f(U_I, t) = 0; \quad J(0, t) = 2J(U_I, t) \quad \text{E 1.1-16}$$

These conditions imply that every electron that reaches the energy U_I generates a second electron by impact ionization and leads to two electrons at zero energy. The second of these is known as the ‘‘flux doubling’’ condition, mentioned above. This formulation is advantageous if an exponential growth $\exp(\beta t)$ that substitutes $\partial f/\partial t$ by $\beta f(\varepsilon)$ is assumed. The kinetic equation can then be replaced by an eigenvalue equation with β as the eigenvalue (flux-doubling model). The equivalence of the two formulations (the kinetic, diffusion equation and the eigenvalue equation) depends on the impact ionization rate being much larger than the rate at which the band-gap energy is being absorbed. That is,

$$U_I v_i(2\varepsilon + U_I) \gg \sigma_{\max} E^2 \quad \text{E 1.1-17}$$

for small ε . For ultrashort intense pulses, this inequality no longer holds. For example, in fused silica at 1053 nm $\sigma_{\max} E^2 = U_I v_i(1.5U_I)$ at an intensity on the order of 10 TW/cm².

1.1 Energy deposition in laser irradiated materials

Thus, the equivalence of the two formulations cannot be taken for granted, but must be checked.

1.2 Flux-doubling model

The flux-doubling model (see [SFH96] and the reference therein) consists of Eq. E 1.1-9 with $S(\varepsilon, t) = 0$ together with the flux-doubling boundary conditions of Eq. E 1.1-16. The quantity to be evaluated is the electron avalanche rate β . Previous theoretical estimates [SMW81] have been made for constant scattering rates, or by assuming vanishingly small β . Neither of these assumptions is valid in the short-pulse limit. Moreover, the calculation assuming small β used perturbation theory based on the solution of the steady-state equation $\partial J / \partial \varepsilon = 0$ which violates the flux-doubling condition, $J(0) = 2J(U_I)$. Hence, the applicability of this result is not clear.

Under the conditions of the flux-doubling model, the equation E 1.1-9 becomes:

$$\frac{\partial f(\varepsilon, t)}{\partial t} + \frac{\partial J(\varepsilon, t)}{\partial \varepsilon} = S(\varepsilon, t) = 0 \quad \text{E 1.2-1}$$

Assuming a solution of the type,

$$f(\varepsilon, t) = g(\varepsilon) \exp(\beta t) \quad \text{E 1.2-2}$$

$$\frac{\partial f(\varepsilon, t)}{\partial t} = \beta f(\varepsilon, t) \quad \text{E 1.2-3}$$

and employing the equation for current J the following is obtained:

$$\frac{\partial J}{\partial \varepsilon} = -\beta f(\varepsilon, t) \quad \text{E 1.2-4}$$

The equation E 1.1-9 becomes:

$$\beta f(\varepsilon, t) + \frac{\partial}{\partial \varepsilon} \left[V(\varepsilon) f(\varepsilon, t) - D(\varepsilon) \frac{\partial f(\varepsilon, t)}{\partial \varepsilon} \right] = 0 \quad \text{E 1.2-5}$$

By integrating the equation E 1.1-9 with respect to energy it is found:

$$\int \beta f(\varepsilon, t) d\varepsilon + V(\varepsilon) f(\varepsilon, t) - D(\varepsilon) \frac{\partial f(\varepsilon, t)}{\partial \varepsilon} = 0 \quad \text{E 1.2-6}$$

Making use of Eq. E 1.2-4 the result is:

$$-J - V(\varepsilon) \frac{\partial J}{\beta \partial \varepsilon} + D(\varepsilon) \frac{\partial^2 J}{\beta \partial \varepsilon^2} = 0 \quad \text{E 1.2-7}$$

or,

$$D(\varepsilon) \frac{\partial^2 J}{\partial \varepsilon^2} - V(\varepsilon) \frac{\partial J}{\partial \varepsilon} = \beta J \quad \text{E 1.2-8}$$

with the boundary conditions:

$$J(0, t) = 2J(U_I, t) \text{ and } \frac{\partial J}{\partial \varepsilon} = 0 \text{ at } \varepsilon = U_I. \quad \text{E 1.2-9}$$

From Eq. E 1.2-4 one can conclude that J is a monotonically decreasing function of the energy (negative derivative), changing from $2J(U_I)$ to $J(U_I)$ within the conduction band.

For high laser intensities, when losses to the lattice are negligible, we can rewrite Eq. E 1.1-10 as:

$$V(\varepsilon) \cong \frac{\sigma(\varepsilon) E^2(t)}{3} \quad \text{E 1.2-10}$$

So, Eq. E 1.2-8 can be set as:

$$\frac{\partial^2 J}{\partial \varepsilon^2} - \frac{1}{2\varepsilon} \frac{\partial J}{\partial \varepsilon} = \frac{\beta J}{D(\varepsilon)} \quad \text{E 1.2-11}$$

Multiplying Eq. E 1.2-11 with ε and integrating over energy between 0 and U_I ,

$$\int_0^{U_I} \varepsilon \frac{\partial}{\partial \varepsilon} \left(\frac{\partial J}{\partial \varepsilon} \right) d\varepsilon - \frac{1}{2} \int_0^{U_I} \frac{\partial J}{\partial \varepsilon} d\varepsilon - \int_0^{U_I} \frac{\beta \varepsilon J}{D(\varepsilon)} d\varepsilon = 0 \quad \text{E 1.2-12}$$

Integrating by parts, we obtain:

$$\int_0^{U_I} \frac{\partial}{\partial \varepsilon} \left(\varepsilon \frac{\partial J}{\partial \varepsilon} \right) d\varepsilon - \int_0^{U_I} \frac{\partial J}{\partial \varepsilon} d\varepsilon - \frac{1}{2} \int_0^{U_I} \frac{\partial J}{\partial \varepsilon} d\varepsilon - \int_0^{U_I} \frac{\beta \varepsilon J}{D(\varepsilon)} d\varepsilon = 0 \quad \text{E 1.2-13}$$

$$\frac{3}{2} \int_0^{U_I} \frac{\partial J}{\partial \varepsilon} d\varepsilon - \int_0^{U_I} \frac{\beta \varepsilon J}{D(\varepsilon)} d\varepsilon = 0 \quad \text{E 1.2-14}$$

Making use of the boundary conditions E 1.2-9, we obtain:

$$\frac{3}{2} J(U_I) = \beta \int_0^{U_I} \frac{J(\varepsilon) \varepsilon}{D(\varepsilon)} d\varepsilon \quad \text{E 1.2-15}$$

Substituting the maximum and minimum values for the flux J into Eq. E 1.2-15 gives:

1.2 Flux-doubling model

$$\beta = \frac{pE^2}{\int_0^{U_I} \frac{d\varepsilon}{\sigma(\varepsilon)}} \quad \text{E 1.2-16}$$

where $p=0.5$ or 1 corresponding to the limiting values for J . Fortunately, the ε weighting of the numerator in the integral part of E 1.2-15 means that low-energy values (bottom of the conduction band) are relatively unimportant in determining β .

This shows that β is proportional to the laser intensity:

$$\beta = \alpha I$$

This model has been used to develop a straightforward analytical solution for the avalanche rate.

The important physical quantities are n (electron number density) and $\langle \varepsilon \rangle$ (average kinetic energy):

$$n = \int_0^{\infty} f(\varepsilon) d\varepsilon \quad \text{E 1.2-17}$$

$$n\langle \varepsilon \rangle = \int_0^{\infty} \varepsilon f(\varepsilon) d\varepsilon \quad \text{E 1.2-18}$$

Integrating E 1.1-9 over energy using E 1.1-15 and neglecting photoionization in E 1.1-14 we obtain after appropriate substitution and simplifications:

$$\int_0^{\infty} \frac{\partial f(\varepsilon, t)}{\partial t} d\varepsilon + \int_0^{\infty} \frac{\partial J(\varepsilon, t)}{\partial \varepsilon} d\varepsilon = - \int_0^I v_i(\varepsilon) f(\varepsilon) d\varepsilon + 2 \int_I^{\infty} v_i(\varepsilon) f(\varepsilon) d\varepsilon \quad \text{E 1.2-19}$$

The current term vanishes as well as the first term on the right-hand side. That means:

$$\frac{\partial n}{\partial t} = \int_I^{\infty} v_i(\varepsilon) f(\varepsilon) d\varepsilon = \langle v_i \rangle n \quad \text{E 1.2-20}$$

Similarly, multiplying with ε and then integrating,

$$\int_0^{\infty} \varepsilon \frac{\partial f(\varepsilon, t)}{\partial t} d\varepsilon + \int_0^{\infty} \varepsilon \frac{\partial J(\varepsilon, t)}{\partial \varepsilon} d\varepsilon = - \int_0^I \varepsilon v_i(\varepsilon) f(\varepsilon) d\varepsilon - U_I \int_I^{\infty} v_i(\varepsilon) f(\varepsilon) d\varepsilon$$

$$\int_0^{\infty} \varepsilon \frac{\partial f(\varepsilon, t)}{\partial t} d\varepsilon + \int_0^{\infty} \frac{\partial}{\partial \varepsilon} (\varepsilon J) d\varepsilon - \int_0^{\infty} J d\varepsilon = - \int_0^I \varepsilon v_i(\varepsilon) f(\varepsilon) d\varepsilon + U_I \int_I^{\infty} v_i(\varepsilon) f(\varepsilon) d\varepsilon \quad \text{E 1.2-21}$$

$$\frac{\partial(n\langle\varepsilon\rangle)}{\partial t} = \int_0^\infty \left[\left(\sigma + \frac{2}{3} \varepsilon \frac{\partial\sigma}{\partial\varepsilon} \right) E^2 - U_{phon} \gamma \right] f(\varepsilon) d\varepsilon - U_I \int_0^\infty v_i(\varepsilon) f(\varepsilon) d\varepsilon = \left(\langle\sigma\rangle E^2 - U_{phon} \langle\gamma\rangle - U_I \langle v_i \rangle \right) n$$

The corresponding equations for the flux-doubling model are similar, except for the impact ionization term, which is replaced by the boundary conditions. Thus, it is expected that $J(0)$ is smaller for the full kinetic equation than for the flux-doubling model.

We have to note that Eq. E 1.2-21 looks formally like the simple Drude theory used to describe electron energy gain by Joule heating and loss by transfer to the lattice, but the effective transport coefficients, such as:

$$\langle\sigma\rangle = \frac{\int_0^\infty \left(\sigma(\varepsilon) + \frac{2}{3} \varepsilon \frac{\partial\sigma(\varepsilon)}{\partial\varepsilon} \right) f(\varepsilon) d\varepsilon}{\int_0^\infty f(\varepsilon) d\varepsilon} \tag{E 1.2-22}$$

depend on averaging over the non-Maxwellian distribution function $f(\varepsilon)$. When exponential avalanche growth occurs, the shape of $f(\varepsilon)$ remains unchanged and $\langle\sigma\rangle$ is time independent.

For the clarity of the demonstration, the assumptions and approximation made should be recapitulated:

- In the avalanche process the excess energy is equally divided between the two electrons involved in the collisions.
- The equivalence of the two formulations (the full kinetic equation and the flux-doubling model) depends on the impact ionization rate being much larger than the rate at which the band-gap energy is being absorbed.
- A temporal exponential growth for the electron density number f has been assumed

Two different behavioral regimes can be distinguished:

For low-intensity long duration pulses it is possible to have a balance between the energy gain and loss (the first two terms on the right-hand side of the last equation from the group E 1.2-21). In this case, the few initial electrons in the conduction band cannot gain enough energy to initiate an avalanche. The energy absorbed by these electrons from the external field is used not to excite more electrons into the conduction band but it is transferred directly into the lattice (the free-electron heating regime). In the long-pulse regime, the source of initial seed electrons can be local defects or impurities. The damage occurs due to high lattice temperatures causing fracture or melting.

1.2 Flux-doubling model

At high laser intensities, the energy absorbed from the field cannot be transferred to the lattice as fast as it is deposited in the electrons. In this case, the absorbed energy is used to feed the avalanche. The average energy per electron is high but remains fixed.

An estimation of the frontier intensity I_b , between the long- and short- pulses can be made on the basis of Eq. E 1.2-21. Initially all electrons are concentrated near the bottom of the conduction band and the derivative term in Eq. E 1.2-21 is small and $\sigma(\varepsilon)$ and $\gamma(\varepsilon)$ can be evaluated at zero energy. The condition for avalanche dominated regimes is:

$$\sigma(0)E^2 \geq U_{phon} \gamma(0) \quad \text{E 1.2-23}$$

For fused silica this gives $I_b=80 \text{ GW/cm}^2$, that means t_b about 60 ps at a fluence of 5 J/cm^2 .

For pulse durations much smaller than t_b the temperature of the lattice can be considered constant and $\sigma(\varepsilon)$ and $\gamma(\varepsilon)$ unchanged during the pulse.

1.3 Solutions of the kinetic equation

The transport scattering rates depend on various types of phonon interaction

Some results are summarized in Arnold, Cartier, and DiMaria [ACD92], which gives a good account of electron scattering in fused silica.

It has been assumed [SFH96 and references therein] that during the avalanche the electron distribution grows in magnitude exponentially without changing shape. At constant laser intensity we have:

$$f(\varepsilon, t) = g(\varepsilon) \exp(\beta t) \quad \text{E 1.3-1}$$

with a stationary but non-Maxwellian distribution

It has been shown above that, under the conditions of the flux-doubling model (E 1.2-16):

$$\beta = \frac{pE^2}{U_l \int_0^{\infty} \frac{d\varepsilon}{\sigma(\varepsilon)}} = \alpha I \quad \text{E 1.3-2}$$

with p -a numerical factor between 0.5 and 1 and $I \propto E^2$.

Typical values for α are about $0.01 \text{ cm}^2 \text{ ps}^{-1} / \text{GW}$ [SFH96].

Based on the numerical calculations in [SFH96] (the avalanche is established extremely quickly, within a few femtoseconds) the solution in the case of a time-varying pulse shape $I(t)$ has the form:

$$f(\varepsilon, t) = g(\varepsilon) \exp\left(\int \beta t\right) \quad \text{E 1.3-3}$$

with $\beta = \alpha I$ holding throughout nearly the entire pulse.

Strictly speaking, the scaling of the distribution function $f(\varepsilon)$ and the current $J(\varepsilon)$ with intensity as well as the proportionality $\beta = \alpha I$ are assured only if the flux-doubling boundary conditions are valid. In addition, the average electron energy $\langle \varepsilon \rangle$ is independent of intensity under these conditions. The impact ionization terms in Eq. E 1.1-15 formally spoil the scaling. However, the number of electrons with energy above U_I remains relatively small and there does not appear to be much effect on β . With impact ionization explicitly accounted for, $\langle \varepsilon \rangle$ increases with increasing intensity but the values for α are almost equal in the two models and also the intensity dependence for $J(\varepsilon)/nI$ is not extremely strong.

So, with the proportionality between β and I and the exponential growth in E 1.3-3, we can rewrite Eq. E 1.3-3.

$$\frac{df}{f} = \beta dt \quad \text{E 1.3-4}$$

So,

$$\frac{dn}{dt} = \beta n = \alpha I(t)n \quad \text{E 1.3-5}$$

Reintroducing the multiphoton ionization $R_{pi}(\varepsilon, t)$ in the source term $S(\varepsilon, t)$ in Eq. E 1.1-9 we can write:

$$R_{pi} = P(I)F(\varepsilon) \quad \text{E 1.3-6}$$

where $P(I)$ is the multiphoton ionization rate and $F(\varepsilon)$ is the distribution function normalized, so that $\int F(\varepsilon)d\varepsilon = 1$.

Photoionization can be treated according to Keldysh theory [Kel65] (being sensitive to the Keldysh parameter $z = \omega (2mU_I)^{1/2} / eE$) in both cases: $z \gg 1$ multiphoton ionization (the electron has time for many oscillations in the binding potential before being ionized) and $z \ll 1$ tunneling respectively (in the case of extremely short intense pulses, tunneling through the binding barrier takes place during a time shorter than a laser period).

1.3 Solutions of the kinetic equation

For example, for 1054-nm light and eight photon absorption, the strong field Keldysh formula (for $z \gg 1$, and $U_{effective} = U_{gap} + e^2 E^2 / (4m\omega^2)$) [Kel65] yields for $P(I)$ [SFH96]:

$$P(I) = 9.52 \times 10^{10} I^8 \quad [\text{cm}^{-3} \text{ps}^{-1}] \quad \text{E 1.3-7}$$

This expression is valid in the range of intensities (TW/cm²) used in the ablation experiments where multi-photon/strong field ionization dominates over tunneling processes. Other expressions for the multiphoton ionization rates in fused silica have been derived by Lenzner et al. [LKS98] and Ming Li et al [LMN99] based on experimental fits and are with 2 up to 6 order of magnitudes smaller as compared to the prediction of the Keldysh formula. Results using other authors estimations for 200 fs IR irradiation based on E 1.3-8 are presented in Table 1.3-1 ($n_{cr} = 1.74 \times 10^{21} \text{ cm}^{-3}$).

References	[SFH96]	ApH2000]	[LKS98]	[LMN99]	[TBK99]	[DLK94]
λ [nm]	1053	800	800	800	800	800
$P(I)$ [cm ⁻³ ps ⁻¹]	$9.52 \times 10^{10} I^8$	$1.599 \times 10^{16} I^6$	$6 \times 10^{8 \pm 0.9} I^6$	$3 \times 10^4 I^6$	tunneling	
MPI-order	8	6	6	6		$n_0 \sim 10^{11}$
Method	[Keldysh]	[Keldysh]	Exp. Fit	Exp Fit	[Keldysh]	cm ⁻³
α [cm ² /J]	$\alpha=11$	$\alpha=11$	$\alpha=4 \pm 0.6$	$\alpha=9$		
Decay term	No	No	No	1/60 fs ⁻¹	No	
N_{pulses}	600	-	50	1	1	1
Threshold [J/cm ²]	1.52	0.86	4.68	4.18	3.8	>10

Table 1.3-1 Estimations on the optical damage threshold based on parameters used in literature for 200 fs laser irradiation of fused silica at 1053 nm and 800 nm. The damage threshold criterion is defined by a critical density $n_{cr} = 1.74 \times 10^{21} \text{ cm}^{-3}$. The exact values for the MPI and avalanche rates remain somewhat controversial.

The presence of photoionization perturbs the distribution function. But if the transient time in Eq. E 1.2-20, E 1.2-21 is short in comparison with the typical time for electron density increase due to photoionization, the distribution function will remain close to $g(\epsilon)$. Under these conditions, the avalanche development can be described by a simple rate equation.

$$\frac{\partial n}{\partial t} = \beta(I)n + P(I) \quad \text{E 1.3-8}$$

with:

$$\begin{aligned} \beta(I) &\propto I \\ P(I) &\propto I^n \end{aligned} \quad \text{E 1.3-9}$$

Even for high photoionization rates, the rate equation can be justified as follows. The photoionization is peaked at the center of the pulse, after that it becomes unimportant. These electrons can be considered as seed electrons for the avalanche.

Fig. 1.3-1 illustrates the evolution of electron density produced by a 100 fs, 1053 nm 10.95 TW/cm² pulse incident on fused silica as calculated by Stuart et al. [SFH96] using Eq. E 1.3-8 (the calculation parameters are: $\alpha=0.011$ [cm²/psGW] and $P(I)=9.52 \times 10^{10} I^8$ [cm⁻³ps⁻¹] in the eight photon absorption case). The pulse intensity and electron density produced by photoionization alone are included for reference. Because photoionization is extremely intensity dependent, the electron production takes place principally at the peak of the pulse. After these seed electrons are produced, the critical density is achieved by electron avalanche. The dense electron plasma is produced at the end of the pulse. Only this part of the pulse experiences strong absorption and reflection. The transient reflectivity has been neglected in the simulation. Also, the threshold is more sensitive to the pulse temporal shape for longer pulses where avalanche becomes significant.

An approximate analytical expression can be derived for the optical damage threshold, assuming that multiphoton ionization and avalanche can be temporarily separated. The damage criterion employed is the condition to reach the electron critical density. With these simplifications, the multiphoton ionization (from the valence band or from intrinsic defect states present in the gap) provides the initial density n_0 of seed electrons for the avalanche. Incubation effects can alter the initial number of absorbing sites due to a defect formation process, so the number of electrons seeding the avalanche can be enhanced. This means firstly that MPI can be treated alone (assuming that multiphoton and avalanche ionization can be separated), and that, after the development of the seed population, this can be considered as the border conditions for integration in the rate equation E 1.3-8 with only avalanche acting as a source.

Thus, $n_0 = \int_{-\infty}^{\infty} P(I)dt$ is the total number of electrons produced by multiphoton ionization.

For a Gaussian laser pulse of duration τ_L (FWHM),

$$I(t) = I_0 \exp\left(-4 \ln 2 t^2 / \tau_L^2\right) \quad \text{E 1.3-10}$$

with the corresponding fluence:

$$F = \int_{-\infty}^{\infty} I(t)dt = \frac{I_0 \tau_L}{2} \left(\frac{\pi}{\ln 2} \right)^{1/2} \quad \text{E 1.3-11}$$

and the total number of electrons produced by the avalanche is then approximately given by:

1.3 Solutions of the kinetic equation

$$n = n_0 \exp \left[\int_0^{\infty} \beta dt \right] = n_0 \exp \left[\frac{\alpha I_0 \tau_L}{4} \left(\frac{\pi}{\ln 2} \right)^{1/2} \right] \quad \text{E 1.3-12}$$

We have stressed that damage occurs when the electron density reaches the critical density when substantial absorption takes place in the electron plasma.

The threshold fluence F_{cr} corresponding to the critical density n_{cr} is then given by:

$$F_{cr} = \frac{I_0 \tau_L}{2} \left(\frac{\pi}{\ln 2} \right)^{1/2} = \frac{2}{\alpha} \ln \left(\frac{n_{cr}}{n_0} \right) \quad \text{E 1.3-13}$$

where $2/\alpha=0.15-0.2 \text{ J/cm}^2$ for fused silica [SFH96].

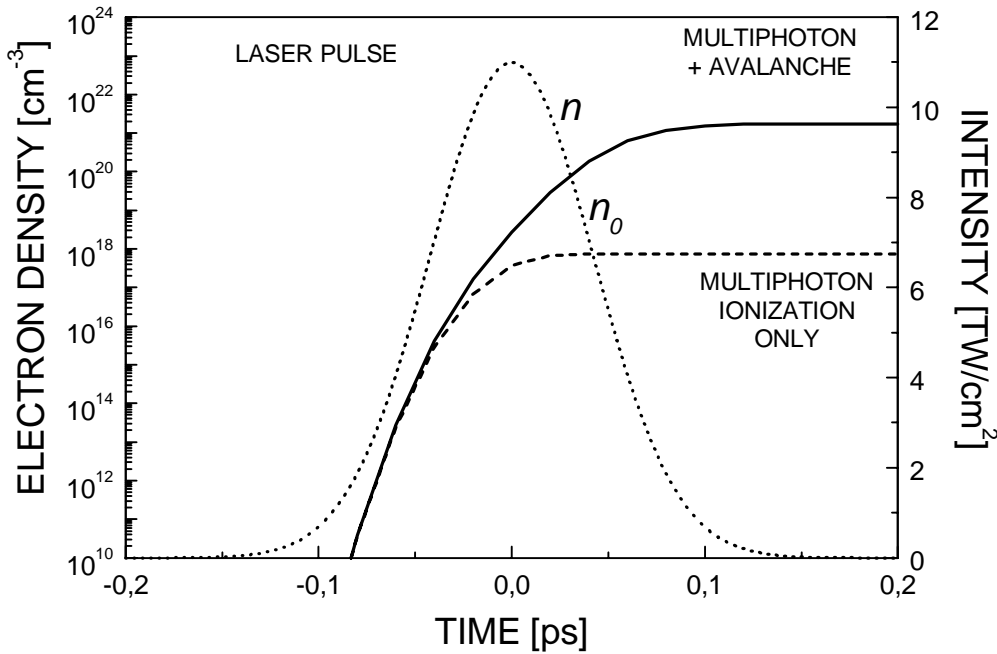


Fig. 1.3-1 Total (solid) and multiphoton produced (dashed) electron densities are plotted along with the Gaussian pulse shape ($I=10.95 \text{ TW/cm}^2$, 100 fs). Seed electrons are produced by multiphoton ionization at the pulse peak after which, at the threshold, an avalanche process produces a critical density $\sim 1.74 \times 10^{21} \text{ cm}^{-3}$. (According to [SFH1996]).

If the number of seed electrons n_0 is independent of intensity (e.g. due to defects) the breakdown threshold F_{cr} would be almost independent of pulse duration. Since n_0 increases rapidly with intensity, at low pulse durations avalanche is becoming less important.

Also, one can see from Eq. E 1.3-13 that for low values for the product $\alpha F_{cr}/2$ the avalanche ionization is not significant i.e. the MPI process alone is sufficient to reach the critical electron density.

Several observations can be made:

- The present argumentation does not take into account the lattice heating and thermal transformation as a criterion for optical damage. The criterion employed is related only to the critical electron density. It is assumed implicitly that absorption at critical density will manifest in the optical damage (by subsequent heat deposition and phase transformation or fracture). Also the transient increasing of the reflectivity was neglected since it becomes effective just at the end of the pulse. For lattice heating different heating formalisms can be employed, either the Drude model [Blo74, SFH96] or a free-electron heating and diffusion model developed by Epifanov [Epi74, ArC92]. Heat transfer to the lattice can be calculated this way.
- The role of multiphoton effects for delivering the seed electrons for avalanche has been outlined by many authors [SFH96, JBC89, DLM96, Ret99]. Evidence for multiphoton effects has been obtained by different experimental techniques such as photoacoustic investigations [JBC89] or photoelectron emission [DGK94] and optical spectroscopy [JGM92], and their suppression has been advocated by Du et al. [DLM96] based on damage thresholds measurements which appeared to be independent of laser polarization. Their quantitative importance has not been completely clarified so far.
- It has to be added that the formalism presented above is truly valid for bulk damage. In the case of surface damage, the presence of structural and morphological defects, inclusions or different types of physical imperfections can result in a decrease of the damage threshold, due to either an increased absorption cross section or field enhancement. It also has to be noted that other highly non-thermal or non-collisional processes can play a role in increasing lattice instability and subsequently leading to optical damage. Some of these processes will be treated in the following sections and they are basically a consequence of a fast electrostatic accumulation of energy.
- The extrapolation of this type of argumentation to multiple irradiation is not evident since accumulation effects have to be considered [JBC89, Mat97] and the role of defects and application of the derived equations in the case of incubation will be presented in Chapter 3. A probabilistic avalanche mechanism would fail to explain the observed reduction in the ablation threshold at repetitive irradiation [JBC89]. In the probabilistic formalism, the statistical nature of the avalanche mechanism is governed by the first one or two ionization sequences, subsequent ionization becoming thus highly probable, with equal probability for each step in the avalanche process. The idea behind it is that if a probabilistic approach is used, then each step in the damaging avalanche process would imply a critical field large enough to make the probability unity and the multiple shot

1.3 Solutions of the kinetic equation

damage will not occur at power densities below the single shot threshold [JBC89]. Thus a cumulative process has to be considered.

Another observation to be made here is that this model holds for moderate intensities and laser fields (below 100 MV/cm) where the multiphoton regime dominates over tunneling. At higher intensities (and very short pulse durations) the applicability of an avalanche rate linearly scaled with laser intensity is doubtful since the assumption of a constant distribution shape is violated in strong fields [TBK99]. In this case more complicated dependencies for the avalanche ionization rates have been employed and numerical methods were applied [ACD92, TBK99, DLK94].

Regarding the rate equation E 1.3-8 some observation should be made. It has been deduced under the conditions that there are no significant electron population losses during the laser pulse. For materials with strong electron-phonon coupling (e.g. quartz, fused silica, fluorides where electrons are self-trapped on a time scale of few hundreds of fs as compared to sapphire or magnesium oxide where electrons can survive in the conduction band for tens of ps [PDG96]) and for pulse durations longer than a few hundreds of femtoseconds, an electron trapping term should be added [LMN99]:

$$\frac{\partial n(t)}{\partial t} = \beta[I(t)]n(t) + \sum_l R_l I^l(t) + \sigma_m p(t) I^m(t) - n(t) \sum_i \frac{1}{\tau_i} - E(t) \quad \text{E 1.3-14}$$

$$\frac{\partial p(t)}{\partial t} = -\sigma_m p(t) I^m(t) + n(t) \sum_i \frac{1}{\tau_i} \quad \text{E 1.3-15}$$

where $\beta(I) = \alpha I$ is the avalanche rate, $R_l I^l = P(I) = P(I)_{VB} + P(I)_D$ are the multiphoton terms from the valence band and extrinsic or initially present (i.e. induced by previous irradiation) defect states (D_l) ($R_l = \sigma_l N_l$ is the multiphoton rate, σ_l is the multiphoton cross section for the valence band and defect states ionization, N_l is the density of the ionization centers corresponding to an l -order process, I is the laser intensity unaffected by transient reflectivity), $\sigma_m p I^m$ are the multiphoton terms originating from the transient defect population (self trapped excitons/unrelaxed Frenkel pairs with the density $p(t)$) that builds up during the pulse duration, τ_i are the characteristic times for recombination, trapping, etc. $E(t)$ represents the photoelectrons emission term (both direct multiphoton emission and free electron heating), which has significance for surface excitation. An example of the trapping effect on the electron population is given in Fig. 1.3-2.

For sub-ps pulses, when trapping is not important, the critical electron density criterion holds, especially since the threshold values are not very sensitive to variations in the electron

density. For ps pulses when fast and efficient electron trapping can lead to a serious depletion in the free electron population, the breakdown threshold should not be defined as the achievement of a critical excitation density [QSM99]. In this case, free electron heating becomes important as underlined by Jones and coworkers [JBC89] and thermal effects are supposed to play a dominant role.

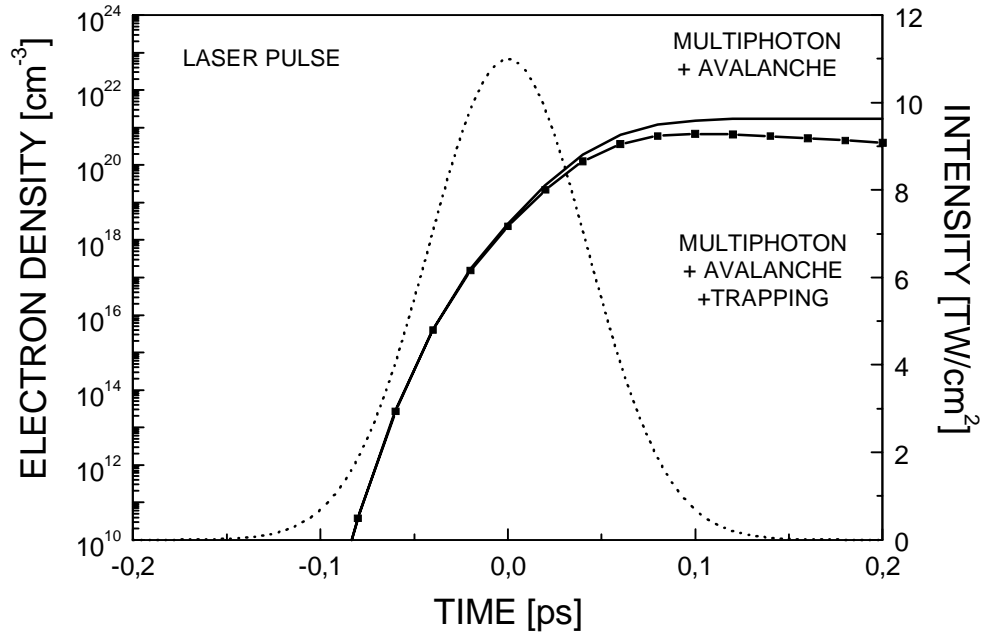


Fig. 1.3-2 Total (solid) and decay corrected (squares) electron densities are plotted along with the 10.95 TW/cm^2 , 100 fs Gaussian pulse shape at 1053 nm for fused silica. Electron characteristic time for being trapped into STE's states is 150 fs [QGM99] (a value of 250 fs is given in [SaG93]). The multiphoton excitation process from the transient defect pair population was neglected, only carrier trapping has been considered.

Applying the formalism used in Eq. E 1.3-10-E 1.3-13, we can write for laser pulse durations comparable with the trapping time τ (i.e. there is no substantial decay in the electron population at the laser pulse end):

$$n \cong n_0 \exp \left[\int_0^{\tau_L} \left(\beta - \frac{1}{\tau} \right) dt \right] = n_0 \exp \left[\frac{\alpha I_0 \tau_L}{4} \left(\frac{\pi}{\ln 2} \right)^{1/2} - \frac{\tau_L}{\tau} \right] \quad \text{E 1.3-16}$$

$$F_{cr} = \frac{I_0 \tau_L}{2} \left(\frac{\pi}{\ln 2} \right)^{1/2} = \frac{2}{\alpha} \left[\ln \left(\frac{n_{cr}}{n_0} \right) + \frac{\tau_L}{\tau} \right] \quad \text{E 1.3-17}$$

Some applications of the above-presented formalism will be given in Chapter 3.

In order to obtain information on the influence of various parameters (multiphoton ionization rate- $P(I)$, avalanche coefficient- α , critical density- n_{cr} , trapping time- $\tau_{trapping}$) in the

1.3 Solutions of the kinetic equation

rate equations: E 1.3-8 and E 1.3-14, and to assess their relative contribution to the optical damage threshold value, sensitivity tests have been performed on the solutions of these equations [ApH2000]. The results are summarized in Table 1.3-2 and give a useful indication on the importance of the accuracy of the input parameters. These results pertain for fused silica at 1053 nm laser irradiation at a critical density of $n_{cr}=1.74 \times 10^{21} \text{ cm}^{-3}$; the nominal parameter values being: $P(I)=9.52 \times 10^{10} I^8 \text{ cm}^{-3} \text{ ps}^{-1}$ and $\alpha=0.011 \text{ cm}^2/\text{psGW}$.

Parameters	$\tau_L=100 \text{ fs}$	$\tau_L=200 \text{ fs}$	$\tau_L=2.8 \text{ ps}$
$P(I)/10$	+14%	+11%	+6%
$10P(I)$	-13%	-11%	-6%
$P(I)/100$	+28%	+23%	+13%
$100P(I)$	-26%	-22%	-13%
$\alpha/2$	+39%	+48%	+69%
2α	-33%	-36%	-42%
$n_{cr}/10$	-13%	-11%	-6%
$\tau_{trapping}=150 \text{ fs}$	+6%	+9%	+69%

Table 1.3-2 Percentage changes in the threshold fluence for laser pulses of different durations at 1053 nm when the input parameters (MPI rate, avalanche rate, critical density and trapping times) vary.

1.4 Lattice heating and thermal processes

If we assume that the thermalization within the electronic system is very fast and that the electron subsystem and the lattice can be characterized by their temperatures (T_e and T_i) the energy can be described by a one-dimensional, two-temperature model [CMN96]

$$C_e \frac{\partial T_e}{\partial t} = -\frac{\partial Q(z)}{\partial z} - g(T_e - T_i) + S$$

$$C_i \frac{\partial T_i}{\partial t} = \nabla(K(T)\nabla T) + g(T_e - T_i)$$

E 1.4-1

$$Q(z) = -k_e \frac{\partial T_e}{\partial z}$$

$$S = I(t)Aa \exp(-az)$$

Here z is the direction perpendicular to the target surface, $Q(z)$ is the heat flux, S is the laser heating source term, $I(t)$ is the laser intensity, $A=I-R$ and a are the surface transmissivity

and the material absorption coefficient, C_e and C_i are the heat capacities (per unit volume) of the electron and lattice subsystems, g is a parameter characterizing the electron-lattice coupling, k_e is the electron thermal conductivity and K is the thermal conductivity of the lattice.

The femtosecond irradiation regime, when the pulse duration is comparable to the electron relaxation time, is characterized by non-significant coupling between the electrons and the lattice. After the laser pulse, the electrons are cooled due to energy transfer to the lattice, and heat conduction to the bulk [CMN96]. For ps pulse durations, the electron temperature becomes quasi-stationary, the losses being compensated by “continuous” laser absorption during the pulse. Heating of the lattice occurs during the laser pulse, although the equilibration with the electron system takes place after the pulse ends. For ns pulses, the electrons and the lattice can be considered in equilibrium for most of the pulse duration. The main source of energy loss is the heat conduction into the solid target. The phase transformation takes place within the pulse duration.

In the case of ablation, the heat-diffusion for the lattice should be solved with appropriate boundary conditions that include phase-transformations (solid-to-liquid, liquid-to-vapor) [vAl87, PDD95] after the initial estimation of the thickness of the homogeneous melted layer.

The two temperatures model is especially valid for metals [Ret1999] since the coupling constant is not energy dependent and electron thermalization takes place in few tens of femtoseconds, so a temperature can be assigned to the electronic system before efficient coupling to the phonons.

A two-system model with different temperatures (the “hot” electrons and the “cold” lattice) should be a good but only qualitative description also for dielectrics, although the temperature source may be difficult to quantify. An additional difficulty arises since electron trapping and recombination constitute additional channels for energy deposition into the lattice besides the electron-phonon coupling. It should be noted that also the electron phonon coupling is highly energy dependent and laser energy absorption is due to take place also by activating the phonon bath due to free electron heating, before electron-ion coupling takes over.

Calculations have been made in the frame of this “thermal spike” model by Toulemonde et al. [TCD96] in the case of swift heavy ion irradiation of dielectrics. Considering that hot free electrons in the conduction band of a dielectric material behave like hot metal electrons,

1.4 Lattice heating and thermal processes

high temperatures (around 3000K for fused silica) have been calculated. The mean electron diffusion length is found to be ~4 nm.

For a detailed understanding of the occurrence of thermal phenomena, a list of most probable thermal processes is given below. The material response to laser radiation is not only controlled by the physics of coupling the laser energy into the material, as we have seen during this chapter, but also by the subsequent dynamics for latent heat transfer in the generation of a liquid-solid interface and vapor plume [PDD95]. Heat conduction in laser irradiated solids is given on a short time scale (determined by electron-electron and electron-phonon thermalization) by electron heat conductivity (electron transport), and, on a longer time scale (longer than electron-phonon coupling time) by bulk thermal conductivity as a parameter describing phonon transport and associated energy redistribution.

As a rule, *thermal* processes occur after establishing a temperature parameter (after a temperature notion can be defined), so after the electron relaxation with the phonons, when the system can be considered to be in a state of local equilibrium.

There are basically four thermal processes to consider:

Normal vaporization

Vaporization from an outer surface is a process, which can operate at basically any pulse length. Nucleation does not enter. The flux of atoms [$\text{atoms cm}^{-2} \text{s}^{-1}$] is governed by the Hertz-Knudsen equation [FuS80, MiK95] describing the surface recession:

$$\left(\frac{\partial x}{\partial t}\right)_{x=0} \approx \eta p_b \exp\left[\frac{\Delta H_v m}{k_b} \left(\frac{1}{T_b} - \frac{1}{T}\right)\right] \times (2\pi m k_b T)^{-1/2} \left(\frac{m}{\rho}\right) \quad \text{E 1.4-2}$$

or the equivalent forms [MiK95, MiK99]:

$$\left(\frac{\partial x}{\partial t}\right)_{x=0} \approx \eta p_{sv} \times (2\pi m k_b T)^{-1/2} \lambda^3 \quad [\text{cm/s}] \quad \text{E 1.4-3}$$

$$\text{Vaporization Flux} \approx \eta p_{sv} \times (2\pi m k_b T)^{-1/2} \quad [\text{particles/m}^2\text{s}] \quad \text{E 1.4-4}$$

where η is the vaporization coefficient (~1), p_b is the “boiling pressure”, (normally similar to 10^5 Pa [MiK95]), p_{sv} –the equilibrium saturated vapor pressure, T_b is the corresponding boiling temperature, λ is the average spacing $\sim(m/\rho)^{1/3}$, ΔH_v is the heat of vaporization (J/g), and it is assumed that there is no vapor present in the ambient and no recondensation. Since the vapor pressure is nonzero at all temperatures exceeding 0 K, it follows that for normal vaporization the surface temperature (T_s) is not fixed. Claims to the contrary, where a “vaporization temperature” (T_v) exists, are therefore wrong [MiK95].

Normal boiling

A second type of process would require that the pulse length is sufficiently long for heterogeneous nucleation to occur, the target undergoes normal boiling from a zone extending from the surface to a depth related to the absorption length or thermal length. In this case, the surface temperature is fixed at T_b and the temperature gradient at and beneath the surface is, by necessity, $\partial T / \partial x \approx 0$. This is so because strong temperature gradients cannot exist among the moving bubbles, which sustain boiling.

Phase explosion (Explosive boiling)

The third type of thermal process requires that the laser fluence is sufficiently high and the pulse length sufficiently short that the target reaches $\sim 0.90xT_{ic}$ (T_{ic} being the thermodynamic critical temperature). In this case homogeneous bubble nucleation occurs (instead of heterogeneous nucleation), and the target makes a rapid transition from a superheated liquid to a mixture of vapor and liquid droplets. The tensile strength of the liquid falls to zero and pressure fluctuations occur. If superheating occurs and the temperature lies sufficiently near T_{ic} , explosive boiling occurs by homogeneous nucleation at a rate of:

$$I_n \approx 1.5 \times 10^{32} \exp\left(-\frac{\Delta G_c}{k_B T}\right) \quad [\text{nuclei/cm}^3 \text{ s}] \quad \text{E 1.4-5}$$

Here ΔG_c is the free-energy change associated with the formation of a spherical critical nucleus. The nucleation rate I_n is significant only for temperatures approaching the critical thermodynamic value [Mar74]. As in the case of normal boiling, phase explosion gives a temperature profile with the form $\partial T / \partial x \approx 0$ at and beneath the surface. At these high temperatures also strong hydrodynamic effects (rarefaction waves [Bul99]) are likely to occur.

Subsurface heating

In the case of normal vaporization, atoms are vaporized from the surface and carry away heat. The target therefore loses the exponential depth temperature profile, and develops in this case a modified profile such that it is hotter beneath the surface. Investigations by Kelly and Miotello [KeM96], [MiK95] on aluminium have demonstrated that this effect has a nonsignificant magnitude.

In all these processes the temperature decays after its peak, due to heat conduction in the sample on the ps up to ns time scale.

